Decomposition of indoor VOC pollutants using non-thermal plasma with gas recycling

Christian Ariane Santos*, Nguyen Hoang Phuong*, Mi Jeong Park*, Sang Bum Kim, and Young Min Jo*,†**

*Department of Environmental Science & Environmental Engineering, Kyung Hee University,
Yongin-City, Gyeonggi-do 17104, Korea
**Green Process and Material R&D Group, KITECH, 31056, Korea
(*Received 8 August 2019 • accepted 12 October 2019*)

Abstract−Volatile organic compounds in the indoor environment of small businesses (painting workshops, hair salons, nail shops, printing shops, laundries etc.) may result in adverse health effects for both workers and customers. Similarly, VOCs identified in these small businesses are included in the list of ozone precursors that harm the environment. We used a non-thermal plasma reactor with gas recycling to study the decomposition of dilute concentrations of VOCs in air. The non-thermal plasma reactor was a surface dielectric barrier discharge (surface DBD) type, and the target gases were methyl ethyl ketone, toluene and n-hexane at concentrations of 20, 50 and 100 ppmv. Highest decomposition efficiency (97%) was achieved by treating n-hexane at 20 ppmv. Gas recycling had an almost negligible effect during pollutant treatment at varying recycling rates (0-50%). Increasing the input energy resulted in higher decomposition efficiency, but had an inverse effect on the energy yield of the system. Concentrations of CO_2 and ozone increased linearly with the increase of energy input in the system. Consumption of ozone for other applications, such as water treatment or coupling the DBD system with an appropriate catalyst, may address this concern.

Keywords: Volatile Organic Compounds, Surface DBD, Gas Recycling, Toluene, MEK, n-Hexane, Indoor Air Pollution, Non-thermal Plasma

INTRODUCTION

Human exposure to indoor air pollutants is increasing, and studies have shown that people are spending an increasingly greater amount of time indoors [1]. Volatile organic compounds (VOCs) are among prevalent indoor contaminants that may damage human respiratory, immune and cardiovascular systems. Most of these VOCs also contribute to environmental damage since they are potentially ozone and smog precursors of photochemical reactions. A recent review paper [2] identified three major indoor environments, namely home, office, and transportation, and the pollutant types, and levels depended on each environment's emission sources. Small businesses such as hair salons, barbershops, nail shops, laundries, printing as well as painting and automotive shops encounter a wide range of VOC species depending on the products and materials used. Table 2 is a list of the highest concentrations of VOCs detected from different business sectors with their ozone formation potential as calculated from another study [3,4].

Among the most studied VOC control technologies is the use of non-thermal plasmas primarily because of their highly chemical reactive environment in which harmful substances are readily decomposed [5]. The high energy electrons and active species (ions, radicals, and excited molecules) generated in the plasma region have shown significant decomposition results in treating a wide variety of pollutants. To determine ideal parameters for an effective non-thermal plasma device, numerous studies on the effect of reactor type, operating conditions, kinetics, reaction mechanisms, discharge type, by-product formations and other parameters have been conducted [6-9]. Removal efficiency for toluene was observed to increase with increased voltage and decreased as the flow rate increased [7]. Different electrode lengths also contributed to VOC degradation but also caused higher ozone production [8], and the use of pure oxygen increased removal efficiency in the degradation of styrene [9].

One type of non-thermal plasma reactor used for decomposition of pollutants is a surface dielectric barrier discharge (DBD) type. A surface DBD type reactor generates highly homogeneous plasma over a large area. The electrodes in the non-thermal plasma reactor have direct contact with each other but surround a dielectric layer, and the discharge propagates on the exposed electrode's surface [10]. With this configuration, active species move from the discharge surface and react with gaseous pollutants at high rates. Varying parameters such as relative humidity, applied power and discharge area have an effect on the performance of a surface DBD reactor [11]. Our previous work [11] showed that 20% relative humidity resulted in the highest decomposition efficiency for toluene, in agreement with other studies [12,13]. Table 1 shows the most common methods currently used for VOC treatment with noted advantages and disadvantages [14].

Based on this empirical background work, our study attempted to identify a more practical design for a surface DBD device that functions with relatively low discharge voltage and frequency (from 3.8 kV and 60 Hz), which would be beneficial in terms of energy consumption. The use of gas recycling aimed to increase the retention times of VOCs and their incompletely decomposed by-products in the plasma zones and chemically active areas to improve

---

Table 1. Brief overview of different VOC control technologies and their limitations [14]

Technology	Removal efficiency (%)	By-product	Strengths	Weaknesses
Absorption	90-98	Wastewater	Able to treat 500 to 5,000 ppm concentrations	Pre-treatment of target compounds is required
			Recovered products may compensate operating cost	Absorption efficiency is affected by the complexity of VOCs
				Tedious maintenance process
Adsorption (Zeolite and activated carbon)	90-96 (zeolite)	Spent zeolite/activated carbon and collected organics	Can still work effectively at RH>90% because selectivity is high for zeolite	Secondary pollution may be emitted during operation
	80-90 (activated carbon)		Recovered products may compensate operating cost	Cost and availability of materials
				Difficult to regenerate for compounds with high boiling point
Bio filtration	60-95	Biomass	Low initial investment cost and less hazardous secondary waste	Takes too much space for the reactor
			Less complex installation and maintenance	Biological parameters require strict monitoring
				Slow and prone to clogging
Catalytic oxidation	90-98	Combustion products and spent catalyst	Up to 70% energy recovery	Susceptible to impurities
			High efficiency with less hazardous by-products than thermal oxidation	Not suitable for gases containing dust impurities
				Catalyst clogging, poisoning or overheating
Membrane separation	90-99	Exhausted membrane	No additional processing needed	Membrane performance is hard to stabilize
			Less energy consumption and less hazardous by-products	Cost and availability of materials
Non-thermal plasma	90-99	Aerosols, ozone, trace gaseous compounds	Beneficial for low concentrations	High energy consumption relative to the treated gas amount
			Non-selective and simple system	
Photo catalysis	90-100	Aerosols, ozone, trace gaseous compounds	Low-cost photo catalyst and sunlight can be used	Reaction rates need to be enhanced 10-100 fold for cost-effectiveness
			Has wider application and is amenable to scale up	
Thermal oxidation	95-99	Combustion products	Up to 85% energy recovery	Releases noxious gases during operation
			Flexible with pollutant type and concentration for the regenerative process	Additional equipment may be required for halogenated compounds

the conversion of the pollutants to CO_2. In particular, correlations of reactor combination and input energy with pollutant decomposition could estimate the energy efficiency of the system. In addition, a new approach to determine the complete conversion of target pollutants was carried out by quantifying the reaction selectivity to CO_2. Although the formation of other by-products aside from ozone was not included in this analysis, the positive impact of gas recycling was measured by tracing the ozone concentration at the efflu-

ent after treatment with and without gas recycling.

MATERIALS AND METHODS

1. Description of the Plasma Reactor

The reactor used in this study was composed of serially arranged DBD cells as illustrated in Fig. 1 [21]. The cylindrical dielectric material was made of glass (thickness 0.8 mm, external diameter 38 mm,

Table 2. List of VOCs detected in various business enterprises in very recent studies

Enterprise	Major VOC	O_3 formation potential	Reference #
Hair salon	Formaldehyde	46-67	[15]
	Isopropyl alcohol	21	
	Ethyl acetate	18	
Barbershop	Toluene	33-45	[16]
	Acetone	35	
Nail shop	Acetone	35	[17]
	Butane	31	
Laundry shop	Toluene	33-45	[18]
	Chlorobenzene	n.a.	
Printing shop	Ethyl acetate	18	[19]
	Isopropyl alcohol	18-23	
	Benzene	10	
Paint/Coating shop	Styrene	5-8	[19]
	Ethyl acetate	18	
Shoe making shop	Acetone	35	[19]
	2-Butanone (MEK)	30-34	
Electronic shop	Toluene	33-45	[20]
	Acetaldehyde	55-62	

n.a. not calculated in the references [18]
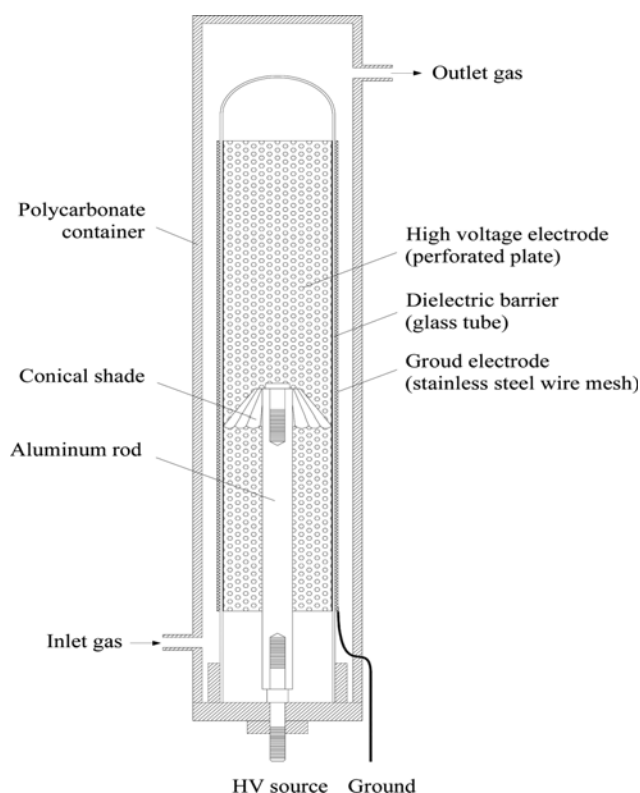
Fig. 1. Parts of the dielectric barrier discharge reactor cell used in this study.

length 240 mm) secured in a plastic base. A 180 mm long perforated aluminum plate coiled inside this glass material acting as the high voltage (HV) electrode and was connected to an aluminum coaxial rod through which electrical power was passed. Wound around the outer surface of the dielectric material was the ground electrode of stainless steel wire mesh (1.7 mm aperture). The tube enclosure (50 mm inner diameter and 260 mm height) was made of polycarbonate material. The inlet and outlet are located approximately 20 mm from the top and base, respectively.

2. Analytical and Electrical Instruments

To measure pollutant concentrations at the inlet and outlet, we used a gas chromatograph coupled with a flame ionization detector (Shimadzu 2010, Japan) [22]. The column used was a Rtx-5 from Restek GC Columns (cat. # 10287). Calibration curves were created for each gas for GC analysis by injecting 5, 20, 50, 100 and 200 ppm of each target gas (toluene, MEK and n-hexane) into the GC to build a linear graph as a concentration readout. Gas samples were purchased in cylinders from Deokyang Co., LTD. Carbon monoxide concentrations were measured using a CO detector (SENKO SP2nd, Korea) supplemented with an electrochemical cell (accuracy of 3%). An infrared gas sensor with a measurement range of 0-2,000 ppm (Gascard NG, Edinburgh Instruments, UK) was used to evaluate the CO_2 level at the outlet. Detector tubes with a measurement range of 4-400 ppm (Gastec No. 18M, Japan) were used to quantify the residual ozone concentration.

The reactor's electrical source was a direct AC power line supplying 220 V at 60 Hz. To measure discharge energy, we followed the Manley method [23] by connecting a capacitor (1 uF) in series with the DBD cells. The discharge voltage was then, measured with a digital oscilloscope (Tektronix TBS2104, Newark, Indiana, USA) equipped with a HV probe (Tektronix P6015A, USA).

3. Experimental Procedure

Fig. 2 illustrates the overall experimental set-up in this study. The purpose of our experiment was to investigate the effect of recycling initially treated gas back to the surface DBD reactor using similar
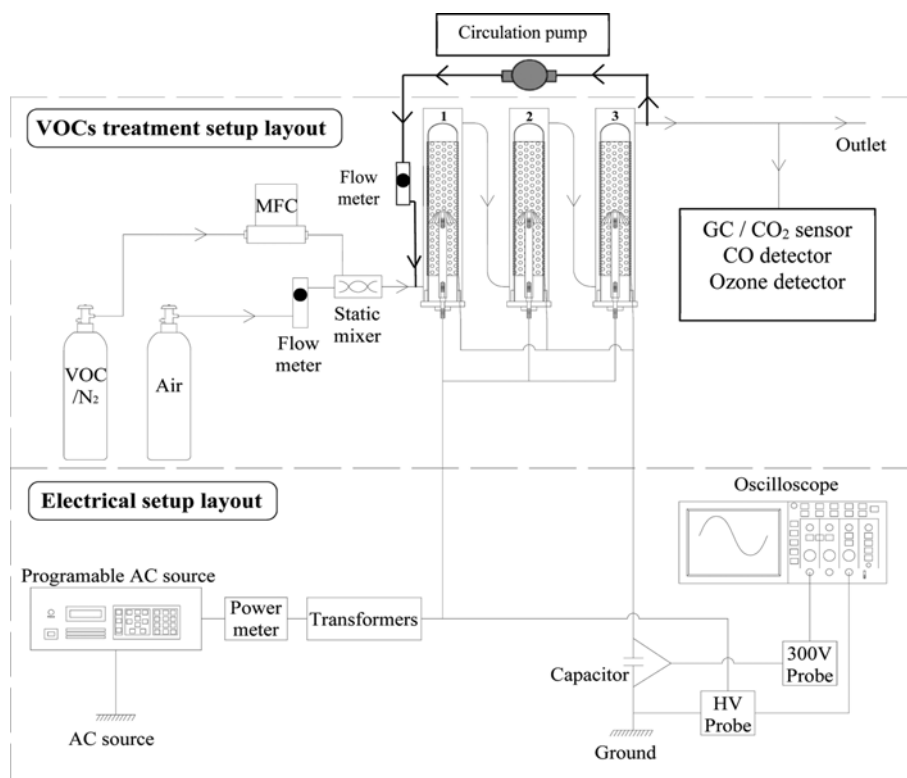
Fig. 2. Experimental layout of the plasma dielectric barrier cells and other components of the study. Gas treatment layout separated from the electrical configuration layout.

operating conditions compared with no gas recycling. This procedure was hypothesized to work in two ways: 1) reprocessing of the target compounds for further reaction, breaking them down into simpler and less harmful compounds, and 2) salvaging reactive species such as ions and radicals, generated inside the reactor to initiate further reactions that can lead to compound degradation.

The concentration of each VOC was kept constant by passing the VOC gas through a mass flow controller with a programmable control box. Calculations were initially made to determine the mass flow controller settings to be input in the control box for each VOC. The background gas in this experiment was synthetic dry air which was controlled by an airflow meter (KOFLOC, Japan)

that was adjusted to give an overall flow rate of 1 L/min. Both VOC and synthetic air were passed through a static mixer to ensure homogeneity of the mixture, which was then injected into a gas chromatograph (GC) for concentration analysis. These procedures were repeated four to five times or until a constant GC concentration reading was achieved for 10, 20, 50 and 100 ppm.

For the experiment without gas recycling, the surface DBD was turned on for 15 minutes' treatment time, in which VOC passed through it once and exited via the exhaust. A sample from the effluent immediately after the 15 minutes of treatment was injected into the GC for a concentration reading, whereas CO_2 concentration was recorded in real-time throughout the duration that the reac-

Table 3. Parameters and conditions used in this study

Parameter	Value and domain	
	No circulation (Toluene, MEK and n-Hexane)	With circulation (n-Hexane)
Temperature	Room temperature (293 K)	Room temperature (293 K)
Pressure	Atmospheric pressure (1 atm)	Atmospheric pressure (1 atm)
Relative humidity	Dry	Dry
Applied voltage	2.9-4.3 kV	2.9-4.3 kV
Applied frequency	60 Hz	60 Hz
Gas flow rate	1 L/min	1-2 L/min
Circulation rate	n.a.	50-90%
Inlet concentration	20, 50, 100 ppmv	10 ppmv

n.a. not applicable

tor was in operation by the CO_2 sensor (Gascard NG, Edinburgh Instruments, UK) directly connected to the outlet through a by-pass tube. CO and ozone were measured by collecting gas samples at the effluent into two tedlar bags; one bag was used for CO concentration measurement by directly pumping out the gas from the bag to the CO sensor (SENKO SP2nd, Korea) and the other sample was used for ozone analysis using Gastec tubes. With gas recycling, the same treatment time was applied, except the gas pump (YKL Tech, Korea) was also turned on during the treatment such that gas from the effluent was directed back into the reactor before being directly injected into the GC for concentration analysis. The same procedures were used to obtain CO_2, CO, and ozone concentrations in this experimental set-up.

Table 3 shows the list of experimental conditions used in this study with and without recirculation. The variables in this experiment were specific energy density, energy yield and recycling rates. A normal input voltage of 220 V at 60 Hz was used in this experiment but through the transformer where the reactors were mounted, the voltage could be stepped-up at five different levels ranging from 2.95 to 4.30 kV. By modifying the transformer level and setting up different reactor combinations, specific energy density values were obtained as shown in Table 4. The energy yield achieved in this study ranged from 1 to 11 g/kWh and was calculated using Eq. (5)

Table 4. Input energy and discharge power combinations used in this study along with the resulting specific energy values

Condition	Reactor 1	Reactor 2	Reactor 3	SED (J/L)
1	3.4 kV	-	-	50
2	4.3 kV	-	-	119
3	4.1 kV	4.1 kV	-	160
4	4.1 kV	4.1 kV	4.1 kV	207
5	4.3 kV	4.3 kV	-	216
6	4.3 kV	4.3 kV	4.3 kV	282

of the calculation section [Materials and Methods. Section 4]. Recycle rates were calculated by multiplying the main flow rate with the target recycle percentages such as 50%, 60%, or 70%. The results were assigned as the flow rate value of the second airflow meter placed after the pump. Each condition was repeated at least twice.

4. Calculations

To calculate decomposition efficiency, we used the following equation:

$$DE(\%) = \frac{[VOC]_b - [VOC]_a}{[VOC]_b} \times 100\% \tag{1}$$

where $[VOC]_b$ is the VOC concentration before treatment and $[VOC]_a$ is the VOC concentration after treatment in ppm.

To calculate CO_2 selectivity, the following definition was used:

$$CS(\%) = \frac{([CO_2]_a - [CO_2]_b) \times 100\%}{n \times ([VOC]_b - [VOC]_a)} \tag{2}$$

where $[CO_2]_a$ is the inlet concentration and $[CO_2]_b$ is the outlet concentration (ppmv). The variable n is the stoichiometric coefficient from the removal reactions, n=7 for toluene, n=8 for MEK and n=6 for n-hexane.

The energy consumption of the system was evaluated based on the specific energy density:

$$SED\left(\frac{J}{L}\right) = \frac{60 \times P}{Q} \tag{3}$$

where,

$$P(W) = E \times F \tag{4}$$

and P is the discharge power of plasma cells (W), Q is the flow rate, E is the discharge energy (J) obtained from Lissajous figures and F is the frequency (Hz).

To determine the energy efficiency of the system, the energy yield was calculated with the following equation:
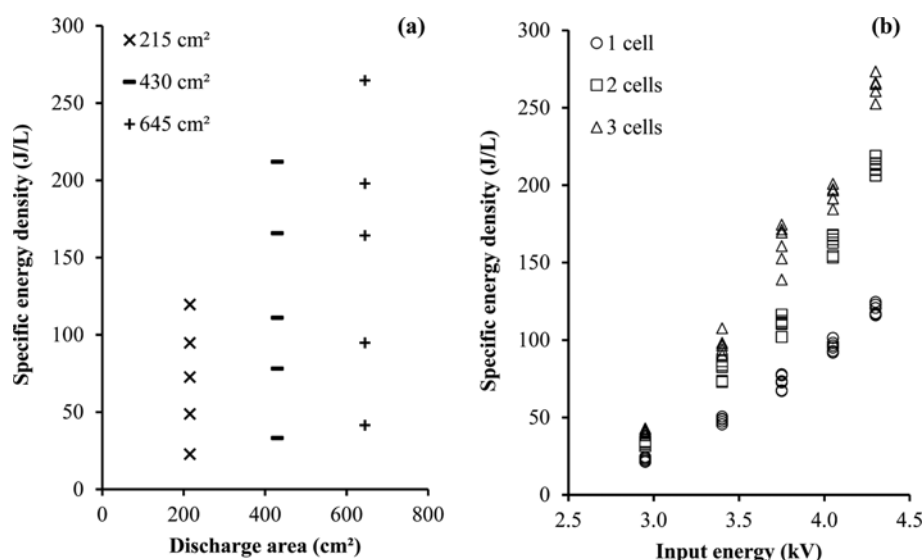
Fig. 3. Calculated specific energy density in terms of (a) discharge area and (b) input energy. Note that one DBD cell is equivalent to 215 cm^2, 2 cells=430 cm^2 and 3 cells=645 cm^2.

$$\text{Energy yield}\left(\frac{g}{kWh}\right)=\frac{[VOC]_b\times DE(\%)\times M\times3.6}{24.04\times SED\left(\frac{J}{L}\right)} \qquad (5)$$

where M is the molecular weight of the VOC (M=92.14 for toluene, M=72.11 for MEK and M=86.18 for n-Hexane).

RESULTS AND DISCUSSION

1. Specific Energy Density

The specific energy density (SED) is the amount of electric power consumed by the DBD reactors during operation. Evaluating this parameter helps determine optimal operating conditions of the DBD reactor series. Varying SED values were obtained by modifying the discharge area and input energy in the system. The discharge areas for one, two and three DBD cells were 215 cm^2, 430 cm^2 and 645 cm^2, respectively. Input energy levels of the system's transformer were in the range of 2.95-4.30 kV.
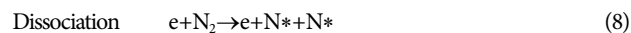
Fig. 3(a) and Fig. 3(b) show the specific energy increased with increasing discharge area and input energy level. Larger plasma discharge areas generated more ions, which subsequently led to increased decomposition of target pollutants due to electron dissociation [24], as shown in Fig. 3(a). Similarly, increasing the discharge area led to an increased SED value, as shown in Fig. 3(b). The final input energy and discharge area combinations used in this study are listed in Table 4.
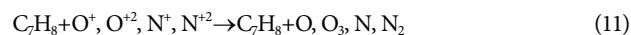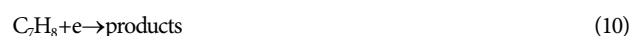
2. Decomposition Efficiency

The target VOCs in this study were toluene, MEK and n-hexane, which were treated separately using a series of DBD cell reactors. Inlet concentrations of the target VOCs were set at 20, 50 and 100 ppmv. The flow rate of the system was 1 L/min and the carrier gas was dry air. Fig. 4 shows the decomposition efficiency for each target pollutant at a constant specific energy density.

As illustrated in Fig. 4, decomposition of VOCs increased as the specific energy density value increased. In dielectric barrier discharges, the discharge energy supplied to the system accelerates electrons, which in turn produce reactive species that react with pollutant molecules (Eq. (6)-(9)).

Ionization $\qquad$ e+N$_2$→2e+N$_2^+$ $\qquad\qquad$ (6)

$\qquad\qquad\qquad$ e+O$_2$→2e+O$_2^+$ $\qquad\qquad$ (7)

Dissociation $\qquad$ e+N$_2$→e+N∗+N∗ $\qquad\qquad$ (8)

$\qquad\qquad\qquad$ e+O$_2$→e+O∗+O∗ $\qquad\qquad$ (9)

The resulting atomic nitrogen and oxygen produced from ionization and dissociation of the background gas by the primary electrons in the dielectric-barrier discharge reactor subsequently oxidize VOCs, forming less harmful compounds or convert them to CO$_2$ and H$_2$O. Considering the abatement of toluene using a stand-alone non-thermal plasma system, the following reaction pathways may be proposed [25]:

C$_7$H$_8$+e→products $\qquad\qquad\qquad\qquad\qquad\qquad$ (10)

C$_7$H$_8$+O$^+$, O^{+2}, N$^+$, N^{+2}→C$_7$H$_8$+O, O$_3$, N, N$_2$ $\qquad$ (11)

C$_7$H$_8$+e→C$_6$H$_5$+CH$_3$ $\qquad\qquad\qquad\qquad\qquad$ (12)

C$_7$H$_8$+OH→C$_7$H$_7$+H$_2$O $\qquad\qquad\qquad\qquad\qquad$ (13)

C$_7$H$_8$+O→C$_7$H$_7$O+H $\qquad\qquad\qquad\qquad\qquad$ (14)

C$_7$H$_8$+O$_3$→C$_7$H$_6$O$_2$+H$_2$O $\qquad\qquad\qquad\qquad$ (15)

C$_7$H$_8$+O$_3$→C$_7$H$_3$O+CO$_2$ $\qquad\qquad\qquad\qquad$ (16)

For these reactions to proceed, an energy requirement capable of breaking molecular bonds of the target VOCs is necessary. Several studies have determined the minimum energy requirements to break each type of chemical bond [26]. In the case of toluene, which has alternating C=C bonds in a ring, 5.5 eV is the minimum energy required to disrupt the C=C ring connections. As for MEK, which contains a carbon-oxygen double bond, the minimum energy required is 7.7 eV, and for single bonded molecules, the required energy begins 3.6 to 4.3 eV.
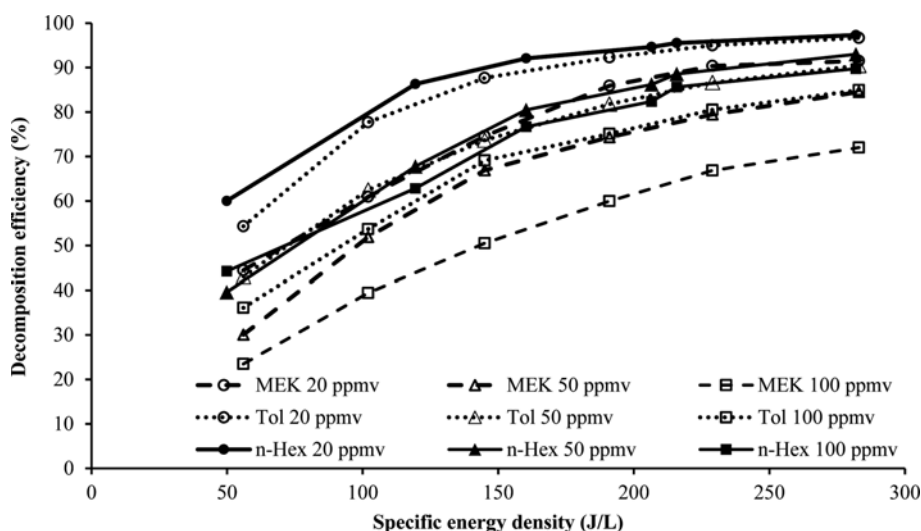

Fig. 4. Decomposition efficiency as a function of specific energy density for MEK, toluene and n-hexane at different inlet concentrations (Q=1 L/min, frequency=60 Hz, carrier gas=dry air).
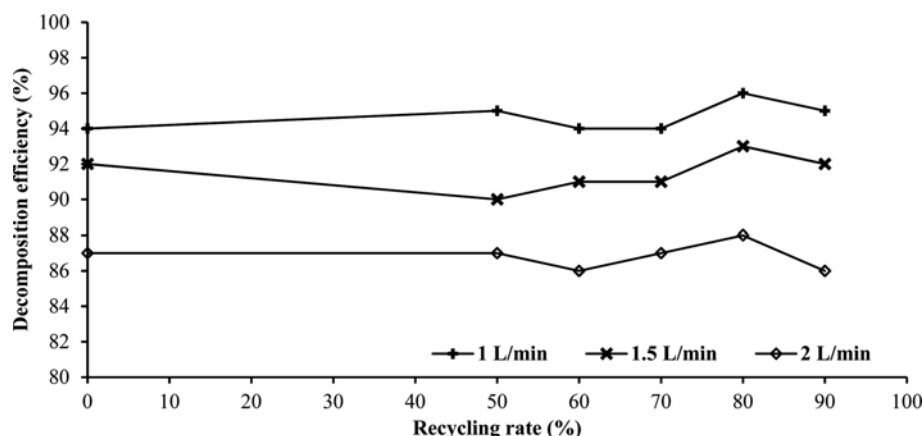
Fig. 5. Decomposition efficiency of n-hexane at different flow rates and recirculation rates (concentration=10 ppmv, input energy=4.3 kV, frequency=60 Hz, carrier gas=dry air).
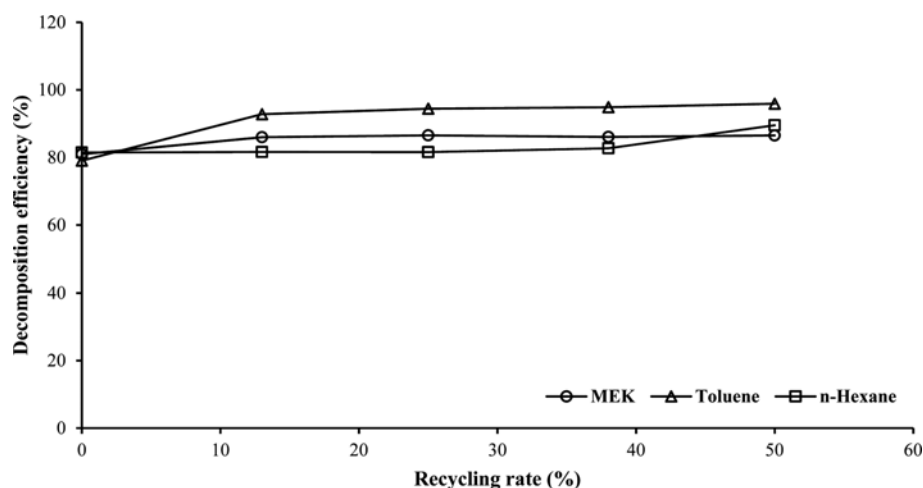

Fig. 6. Decomposition efficiency of different VOCs in this study at varying recycling rates (concentration=20 ppmv, input energy=4.3 kV, frequency=60 Hz, carrier gas=dry air).

The maximum decomposition efficiency of the system for each treated gas was as follows: n-hexane (97%), toluene (96%) and MEK (92%). In another study [27], n-hexane was more easily decomposed than toluene and MEK. The simpler molecular structures of n-hexane (C-C and C-H bonds) are more easily broken than the more complex structures of toluene and MEK [28]. This indicates that compound structure has an effect on the decomposition performance of the DBD system. The Karatum and Deshusses study calculated the reaction rate constants k of each compound, and their results were n-hexane (k=0.0076), toluene (k=0.0033) and MEK (k=0.0018). Despite the different molecular structures and energy requirements of the representative VOCs treated in this study, the surface DBD reactor used exhibited good flexibility and multi-functionality in treating low concentrations of volatile organic compounds.

To determine the effect of gas recycling on the decomposition efficiency of a VOC, we performed a two-part experiment, first with only n-hexane as the target gas at different flow rates and second with all the gases at a fixed concentration of 20 ppmv and different recycling rates. For the first part with only n-hexane as the pol-

lutant, we achieved the highest decomposition efficiency (96%) at 1 L/min, with a gas recirculation rate of 80% (Fig. 5). Similarly, at other flow rates, recirculation of the treated gas back to the system after initial passage at a rate of 80% of its original flow yielded the highest decomposition efficiency. In the second part of the experiment, we observed that gas recycling did not provide a significant contribution to the decomposition results (Fig. 6). Addition of the gas recycling device in the set up helped re-introduce active radicals and other species inside the reactor, thus, increasing contact probability, but also reduced the residence time of the target gas from remaining long enough inside the plasma device for the proper reactions to take place, resulting into almost the same degradation rate. However, recycling of the gas back to the reactor helped reduce the detected ozone concentration at the outlet as can be observed in Fig. 10.

3. Energy Efficiency

The energy efficiency of the system, defined as the amount of pollutant decomposed per input energy in Eq. (5), showed an inverse relationship with decomposition efficiency. Treatment of different VOCs at 100 ppmv (Fig. 7(a)) indicated n-hexane gave the highest
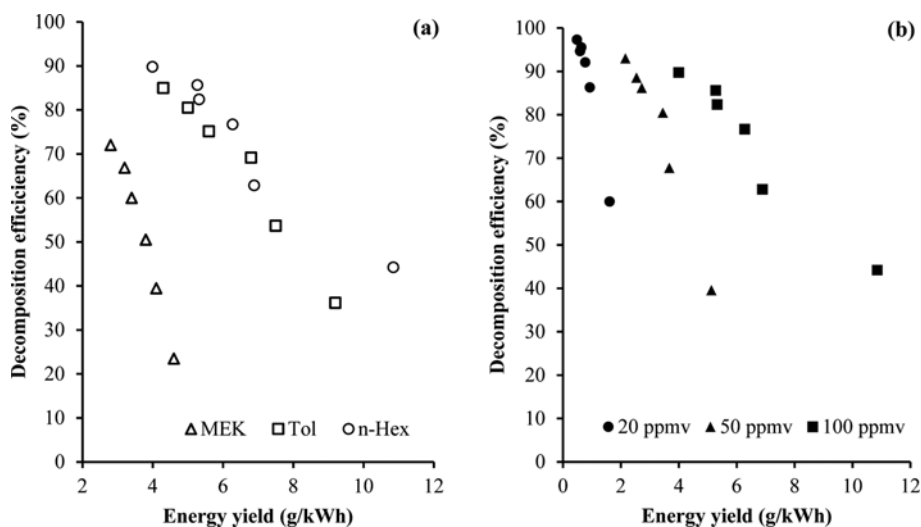
Fig. 7. Decomposition efficiency as a function of energy yield (a) as per pollutant type at 100 ppmv and (b) per varying concentration using n-hexane as target gas.
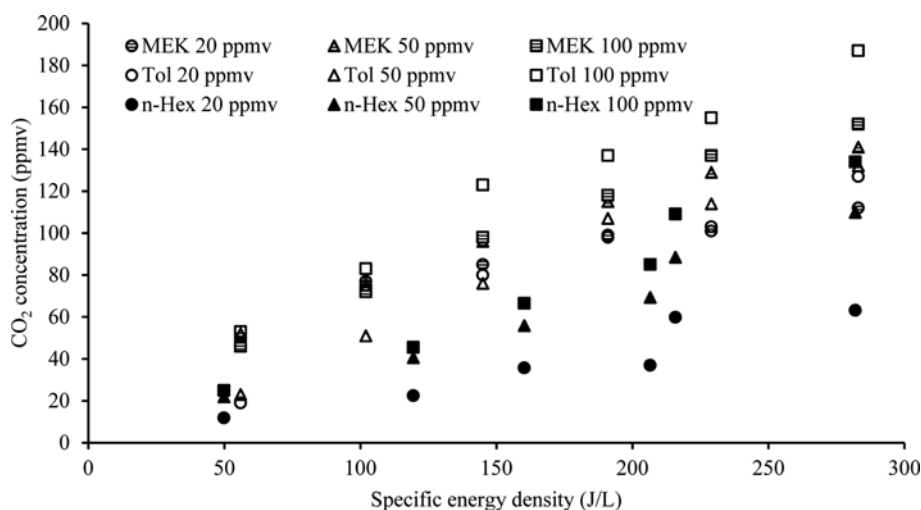

Fig. 8. CO₂ concentration after treatment as a function of specific energy density for MEK, toluene and n-hexane at different concentrations.

energy yield, since more n-hexane was decomposed than MEK and toluene at the same input energy level. The energy yield of n-hexane treated separately at different concentrations (Fig. 7(b)) was more favorable when the VOC concentration was higher. Nonetheless, the serial DBD system used in this study is appropriate to treat dilute concentrations of VOCs at 100 ppmv and lower.

4. CO₂ Selectivity and Ozone

An indication of complete VOC destruction is the presence of CO_2 at the outlet after a certain treatment period. As shown in Fig. 8, the CO_2 concentration increased proportionally with increasing input energy. Therefore, increasing the input power can lead to more complete decomposition of VOC, but the energy efficiency of the system will likely decrease when treating gasses at lower concentrations. The selectivity for CO_2 was investigated in another study [28] that found coupling of a DBD reactor with quartz dielectric balls resulted in a higher conversion to CO_2 because of a more distributed energy field. Thus, the DBD system used in this study could

be a suitable tool for comprehensive destruction of indoor VOCs.

The presence of ozone in non-thermal plasma systems is unavoidable. As shown in Fig. 9, ozone concentrations increased as the energy supplied to the system was increased. A similar phenomenon of increasing ozone with increasing input power regardless of the carrier gas used has been reported in other research [28]. The dissociation reaction of oxygen with electrons leads to the formation of ozone and limits the energy effectiveness of a plasma device. On the other hand, during treatment of VOCs with recycling, the ozone concentration was observed to decrease as the recycling rate was increased (Fig. 10). Rostami et al. stated that ozone may remain up to three days in the gas phase under natural conditions, but its lifetime as well as other radicals can be reduced if the air contains reactive organic molecules such as benzene and would not emerge from the gas stream [30]. Recent studies of ozone-catalytic decomposition of dilute concentrations of VOCs have shown promising usage for ozone produced in a non-thermal
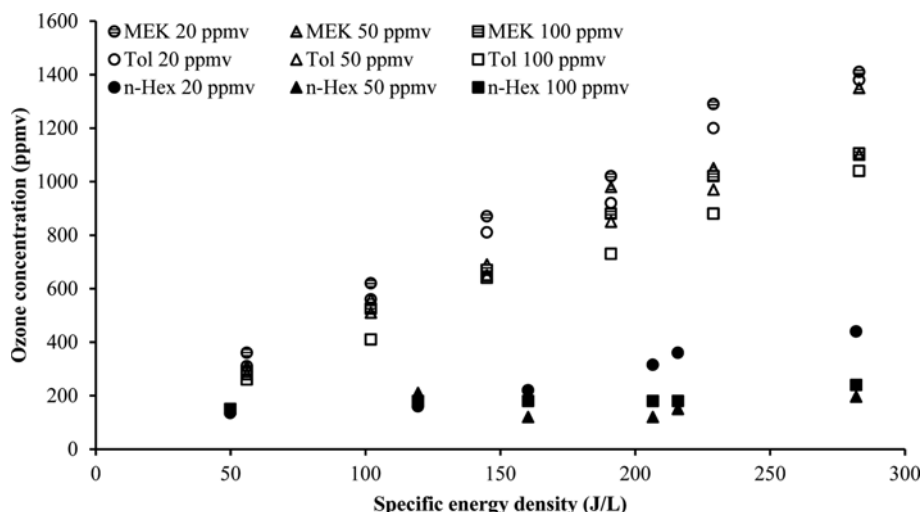
Fig. 9. Ozone concentrations at the outlet (in ppmv) as a function of specific energy density for MEK, toluene and n-hexane at varying concentrations (20, 50 and 100 ppmv).
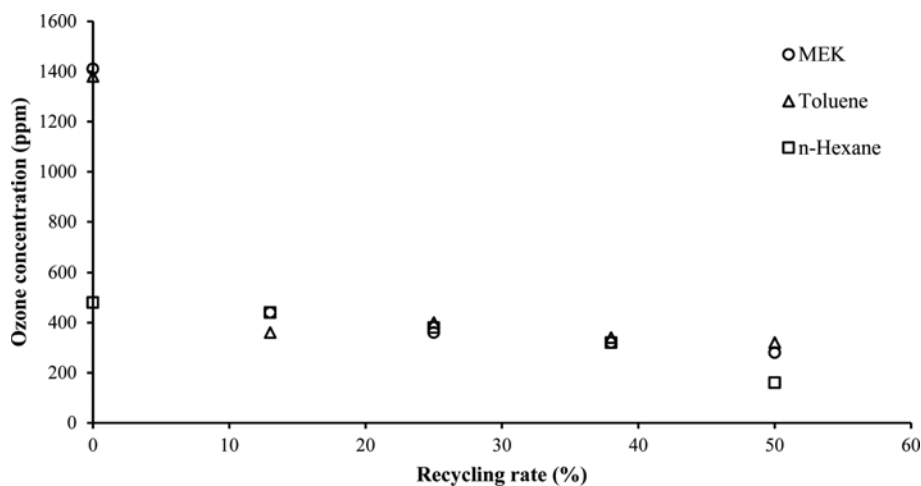

Fig. 10. Ozone concentrations at the outlet (in ppmv) as a function of recycling rate for MEK, toluene and n-hexane at a fixed concentration of 20 ppmv (input energy=4.3 kV, frequency=60 Hz, carrier gas=dry air).

plasma reactor if coupled with a suitable catalyst [31-33].

CONCLUSIONS

Volatile organic compounds exist within indoor air at a low concentration but pose harm to human health and the environment as ozone precursors. Non-thermal plasma is the prevailing indoor air control system used to decompose these unwanted compounds. We used a series of dielectric-barrier discharge reactors and investigated the decomposition efficiency and energy yield, as well as ozone and CO_2 concentrations after VOC treatment.

MEK, toluene and n-hexane were the target gasses diluted with dry air to attain initial concentrations of 20, 50 and 100 ppmv. At the same input energy, n-hexane had higher decomposition efficiency (97%) than MEK (92%) and toluene (96%), indicating that gas type is a significant factor in the performance of a DBD reactor. Using n-hexane as target gas (at 10 ppmv), recirculation of the

gas at different circulation rates provided slight improvement in decomposition efficiency, but the effect was almost negligible. In comparison with other VOC abatement technologies, non-thermal plasma proved to be a feasible technique with respect to ease of operation and low input voltage requirement. The surface DBD design used in this study was equipped with its own transformer that allowed operation with a normal power source (220 V, 60 Hz), which implies that the scalability of this design could be executed more easily than other VOC control systems [34].

CO_2 concentration increased with increased input energy, indicating that higher input power leads to more complete VOC destruction. However, the energy efficiency of the system should be considered when treating pollutants at low concentrations. Other studies have achieved removal efficiencies comparable to our results, such as Karatum and Deshusses [27] who treated MEK, toluene, and n-hexane, resulting in a maximum 90% removal efficiency with 350 J/L specific energy density, while Mustafa et al. [35] recorded a

removal efficiency of 100% in treating toluene but with a higher input energy (up to 65.8 W). Significant ozone concentrations were detected at the outlet of the reactor as a result of electron dissociation. The effects of power source and humidity in the creation of ozone in a dielectric barrier discharge were investigated [36], and with AC as the power supply and increased relative humidity, ozone production efficiency decreased. Future studies considering the use of different power sources and increasing relative humidity in the system may be used. Nonetheless, consumption of ozone for other applications such as water treatment or coupling the DBD system with an appropriate catalyst may address this concern.

ACKNOWLEDGEMENTS

REFERENCES

1. I. Odeh and T. Hussein, *Int. J. Environ. Res. Public Health*, **13**, 960 (2016).
2. W. T. Kwok, *Energy and Buildings*, **130**, 637 (2016).
3. M. E. Jenkin, R. G. Derwent and T. J. Wallington, *Atmos. Environ.*, **163**, 128 (2017).
4. W. Wu, B. Zhao, S. Wang and J. Hao, *J. Environ. Sci.*, **53**, 224 (2017).
5. A. M. Vandenbroucke, R. Morent, N. De Geyter and C. Leys, *J. Hazard. Mater.*, **195**, 30 (2011).
6. M. Ondarts, W. Hajji, J. Outin, T. Bejat and E. Gonze, *Chem. Eng. Res. Des.*, **118**, 194 (2017).
7. P. Liang, W. Jiang, L. Zhang, J. Wu, J, Zhang and D. Yang, *Process Saf. Environ. Prot.*, **94**, 380 (2015).
8. M. Bahri, F. Haghighat, S. Rohani and H. Kazemian, *Chem. Eng. J.*, **302**, 204 (2016).
9. H. Zhang, K. Li, C. Shu, Z. Lou, T. Sun and J. Jia, *Chem. Eng. J.*, **256**, 107 (2014).
10. R. Brandenburg, *Plasma Sources Sci. Technol.*, **27**, 1 (2018).
11. H. P. Nguyen, M. J. Park, S. B. Kim, H. J. Kim, L. J. Baik and Y. M. Jo, *J. of Cleaner Production*, **198**, 1232 (2018)
12. Y. F. Guo, D. Q. Ye, Y. F. Tian and K. F. Chen, *Plasma Chem. Plasma Process*, **26**, 237 (2006).
13. J. Van Durme, J. Dewulf, W. Sysmans, C. Leys and H. Van Lan-
genhove, *Chemosphere*, **68**, 1821 (2007).
14. A. K. Gupta and B. Modi, *J. Inst. Eng. India, Ser. A*, **99**, 565 (2018).
15. C. J. Chang, S. F. Cheng, P. T. Chang and S. W. Tsai, *Indoor Air*, **28**, 173 (2018).
16. M. Ebrahemzadih, S. Sadeghi, P. Mozaffari and H. Salehzadeh, *J. Adv. Environ. Health Res.*, **6**, 67 (2018).
17. M. S. Yoon, Y. J. Choi and H. W. Ryu, *J. of Odor and Indoor Environment*, **15**, 319 (2016).
18. O. H. Park, K. S. Lee, K. W. Min, G. W. Cho, K. J. Yoon, W. S. Jeong, Y. G. Cho, E. S. Kim and J. S. Yang, *J. of Korean Society of Occupational and Environmental Hygiene*, **26**, 159 (2016).
19. J. Zheng, Y. Yu, Z. Mo, Z. Zhang, X. Wang, S. Yin, K. Peng, Y. Yang, X. Feng and H. Cai, *Sci. Total Environ.*, **456-457**, 127 (2013).
20. S. O. Baek, L. Narayana and Y. K. Seo, *Sensors*, **15**, 19102 (2015).
21. L. J. Baik, Plasma Generating Apparatus for Air Cleaning and Sterilizing. KR Patent, 1010037290000 (2010)
22. H. M. McNair, J. M. Miller and N. H. Show, Basic Gas Chromatography, Wiley, New Jersey (2019).
23. T. C. Manley, *J. Electrochem. Soc.*, **84**(1), 83 (1943).
24. H. Huang, D. Ye, D. Y. Leung, F. Feng and X. Guan, *J. Mol. Catal. A Chem.*, **336**, 87 (2015).
25. G. Xiao, W. Xu, R. Wu, M. Ni, C. Du, X. Gao, Z. Luo and K. Cen, *Plasma Chemistry and Plasma Processing*, **34**, 1033 (2014).
26. K. Urashima and J. Chang, *IEE Transactions on Dielectrics and Electrical Insulation*, **7**, 602 (2000).
27. O. Karatum and M. A. Deshusses, *Chem. Eng. J.*, **294**, 308 (2016).
28. Q. Jin, B. Jiang, J. Han and S. Yao, *Chem. Eng. J.*, **286**, 300 (2016).
29. F. Holzer, F. D. Kopinke and U. Roland, *Chem. Eng. J.*, **334**, 1988 (2018).
30. R. Rostami, G. Moussavi, S. Darbari and A. Jonidi Jafari, *Plasma Sci. Technol.*, **21**, 095501 (2019).
31. M. Aghbolaghy, J. Soltan and R. Sutarto, *Chem. Eng. Res. Des.*, **128**, 73 (2017).
32. L. Jiang, G. Nie, R. Zhu, J. Wang, J. Chen, Y. Mao, Z. Cheng and W. A. Anderson, *J. Environ. Sci.*, **55**, 266 (2016).
33. Z. Zhang, Z. Jiang and W. Shangguan, *Catalysis Today*, **264**, 270 (2016).
34. Y. S. Son, *Chem. Eng. J.*, **316**, 60 (2017).
35. M. F. Mustafa, X. Fu, Y. Liu, Y. Abbas, H. Wang and W. Lu, *J. Hazard. Mater.*, **347**, 317 (2018).
36. X. Zhang, B. J. Lee, H. Im and M. S. Cha, *IEEE Trans. Plasma Sci.*, **44**, 2288 (2016).